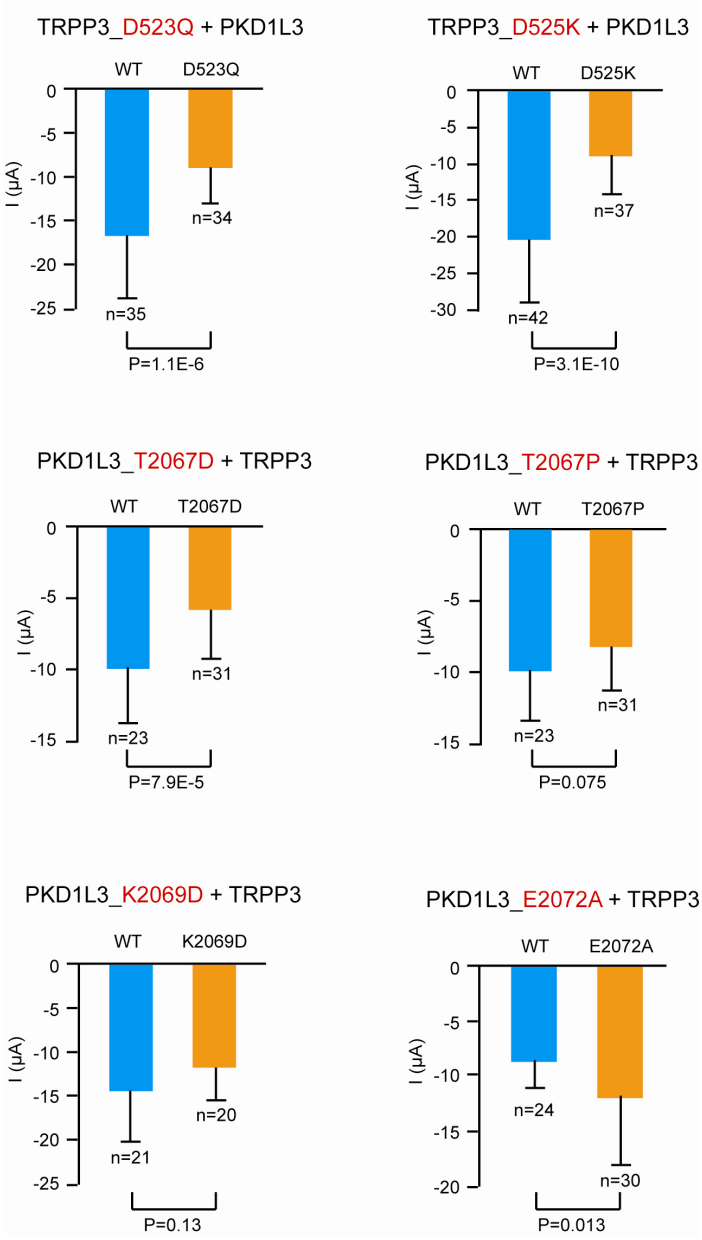

Supplementary Figure S1. Comparison of peak current amplitude of WT and mutant PKD1L3/TRPP3 complexes. Currents were elicited by citric acid (pH 2.8) and were recorded at -80 mV from wild type (blue bars) and six different mutant (orange bars). Bath solution contains 100 mM NaCl, 0.5 mM $MgCl_2$, 2 mM HEPES, pH 7.5. Each panel was obtained from the same batch of oocytes.

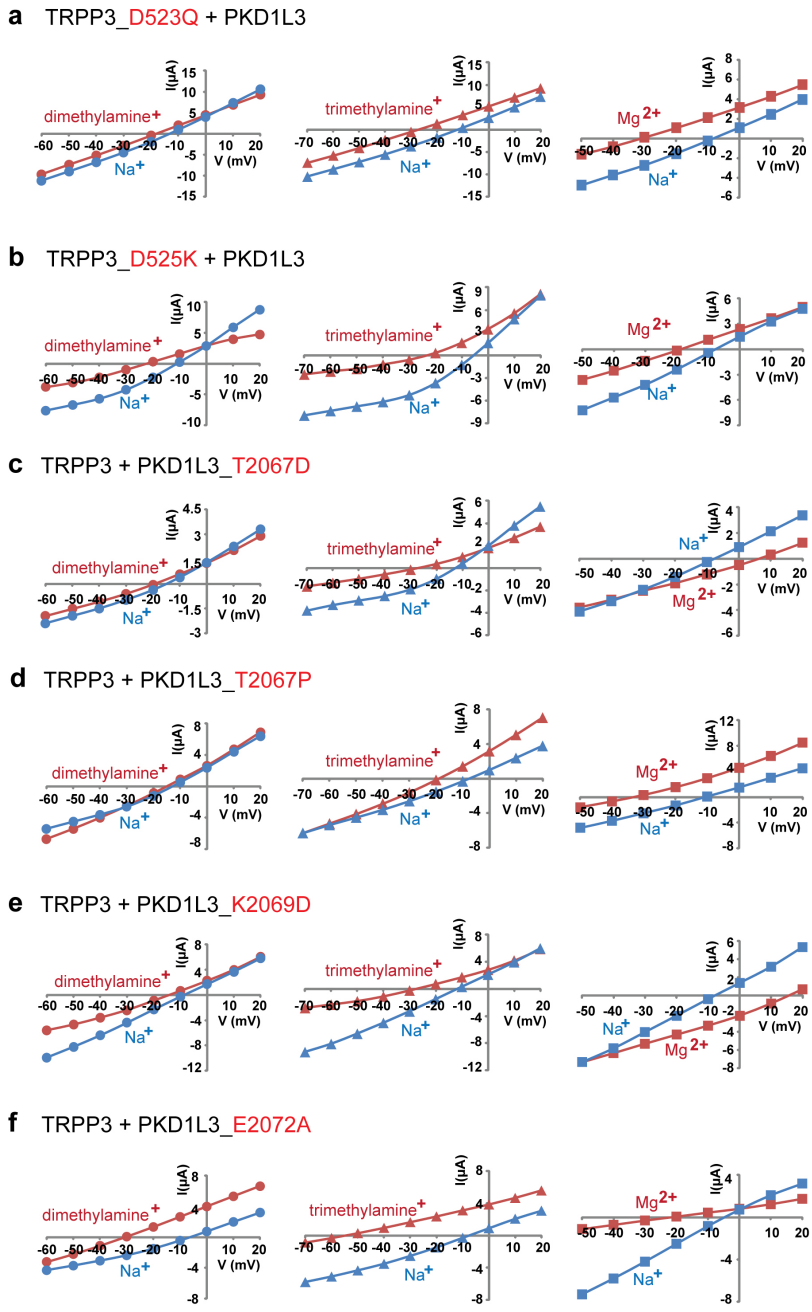

Supplementary Figure S2. Representative I-V curves of acid-induced currents of mutant PKD1L3/TRPP3 complexes. The currents were recorded in a bath solution containing either 100 mM NaCl (blue), or 100 mM dimethylamine·HCl, or 100 mM trimethylamine·HCl, or 70 mM $MgCl_2$ (red). The two I-V curves in each panel were obtained from the same oocyte.

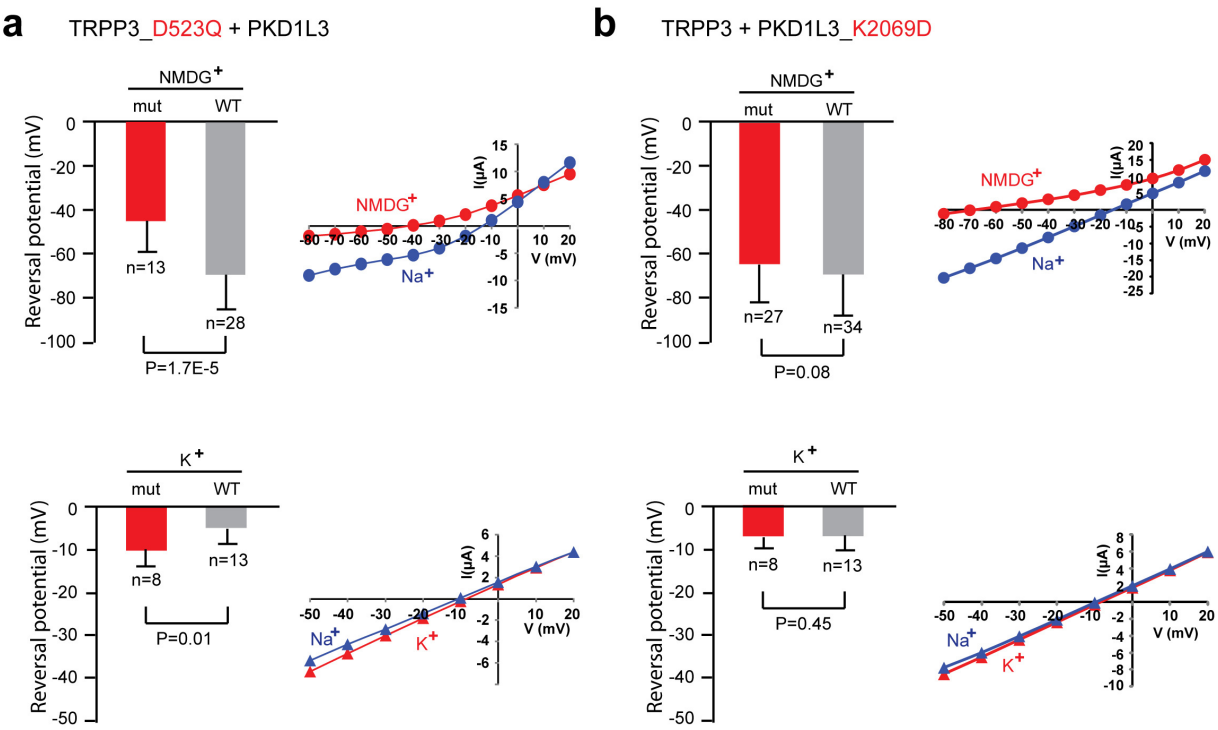

Supplementary Figure S3. Effects of putative pore mutations on the permeability to $NMDG^+$ and K^+. (**a** and **b**) Bar graph showing the reversal potential of currents recorded from WT (grey bars) or mutant (red bars) PKD1L3/TRPP3 complexes (mutation indicated at the top of each panel) in a bath solution containing 100 mM $NMDG^+$, or K^+. All pair-wise data were obtained from the same batch of oocytes. Compared to WT channels, the TRPP3-D523Q mutation significantly changed the reversal potential in $NMDG^+$ and K^+, but the PKD1L3-K2069D mutation did not. Representative I-V curve for each mutant is shown on the side. The currents were recorded in a bath solution containing either 100 mM NaCl (blue), or 100 mM NMDG·HCl, or 100 mM KCl. The two I-V curves in each panel were obtained from the same oocyte.

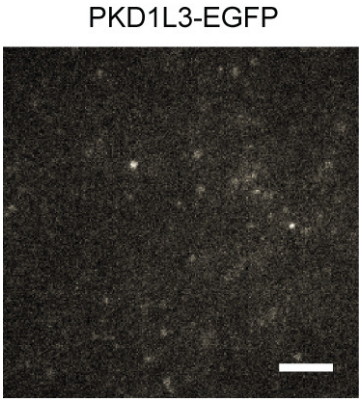

Supplementary Figure S4. PKD1L3-EGFP alone has no surface expression.

Representative TIRF image from an oocyte expressing PKD1L3-EGFP alone, showing that PKD1L3 does not traffic to the cell surface on its own. Scale bar, 2 μm.

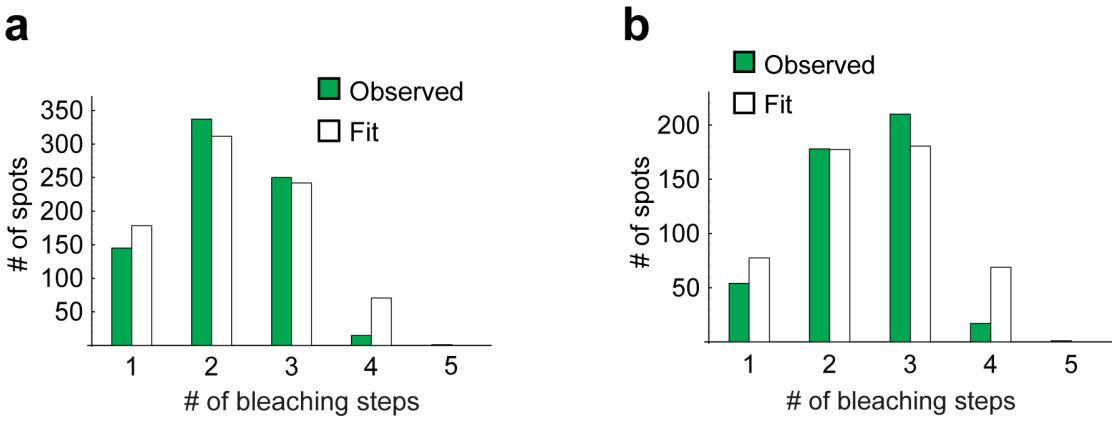

Supplementary Figure S5. Homomeric TRPP3 and heteromeric PKD1L3/TRPP3 complexes do not contain 4 TRPP3 subunits. (**a**) Distribution of observed EGFP bleaching steps (green bars) for TRPP3-EGFP spots on the plasma membrane of *Xenopus* oocytes fits poorly to the calculated distribution (white bars) assuming that 4 EGFP molecules exist in each spot. The best fit was obtained with the probability of GFP to be fluorescent being set to 54%. (**b**) Distribution of observed EGFP bleaching steps (green bars) for PKD1L3-mCherry and TRPP3-EGFP dual-fluorescence spots fits poorly to the calculated distribution (white bars) assuming that 4 EGFP molecules exist in each spot. Best fit was obtained with a 60% probability of GFP being fluorescent.

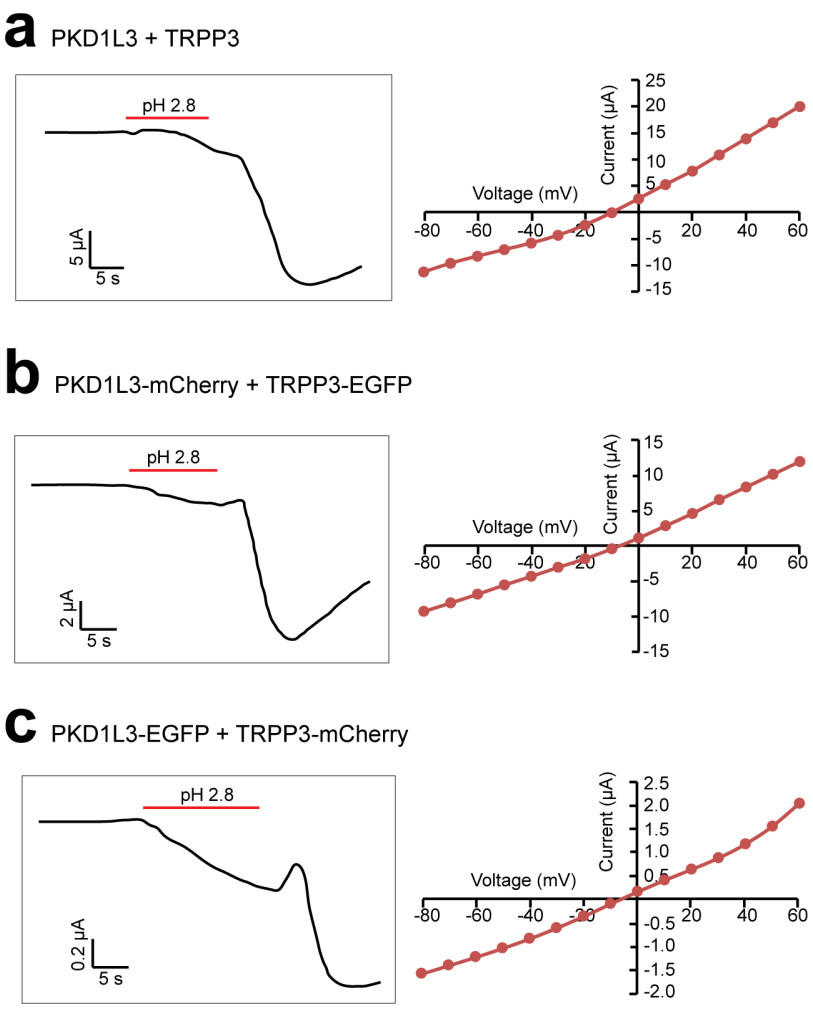

Supplementary Figure S6. EGFP- and mCherry-tagged TRPP3 and PKD1L3 subunits form functional channels. Left panels: representative whole-cell currents in response to extracellular citric acid (pH 2.8, red bar) recorded in oocytes expressing channels formed by WT PKD1L3 and TRPP3 (**a**), PKD1L3-mCherry and TRPP3-EGFP (**b**), or PKD1L3-EGFP and TRPP3-mCherry (**c**). Holding potential = -60 mV. Right panels: I-V curves of acid-induced currents, obtained at the end of the current traces shown on the left.

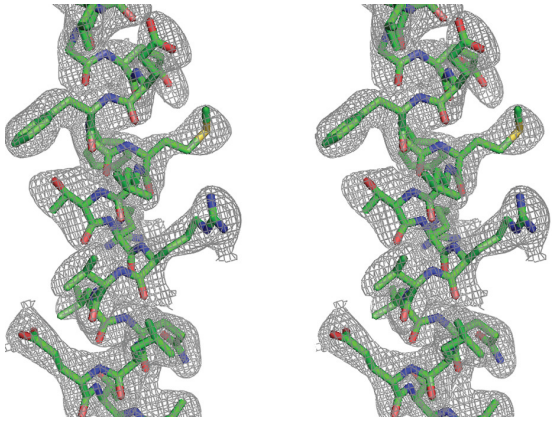

Supplementary Figure S7. Electron density of the TRPP3 coiled-coil domain.

Stereo view of the representative electron density map contoured at 1σ for the N terminal portion of the TRPP3 coiled-coil domain trimer structure. Only a monomer is shown here.

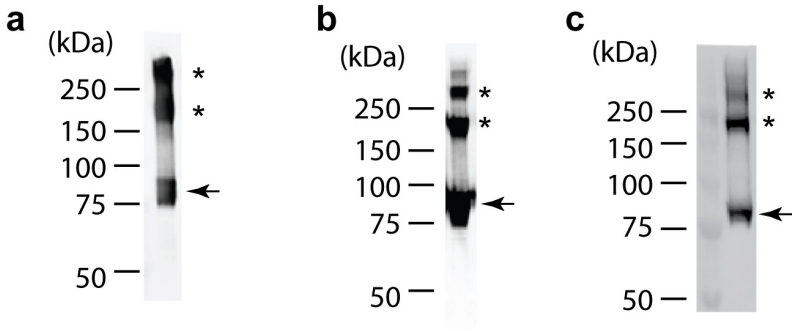

Supplementary Figure S8. Oligomers of TRPP3 on SDS-PAGE. (**a**) Sample was boiled for 3 min with SDS Blue Loading Buffer (New England Biolabs) and 50 mM DTT. Arrow and asterisks indicate TRPP3 monomer and oligomers, respectively. (**b**) Sample was incubated at 37 ℃ for 30 min with SDS Blue Loading Buffer, 50 mM DTT and 5% β-mercaptoethanol. (**c**) Sample was incubated at 37 ℃ for 30 min with SDS Blue Loading Buffer and 8 M urea, 50 mM DTT and 50 mM Tris[2-carboxyethyl] phosphine hydrochloride (TCEP·HCl, Pierce). In this case, the SDS-PAG also contained 8 M urea. Compare to DTT, TCEP is a more stable and more effective reducing agent.

Supplementary Table S1. Permeability ratios of WT and mutant PKD1L3/TRPP3 channels for $NMDG^+$ and K^+.

Channel type	$NMDG^+$		K^+	
	ΔE_{rev} ± SD (n)	P_{NMDG}/P_{Na}	ΔE_{rev} ± SD (n)	P_K/P_{Na}
Wild Type	-60 ± 14.4 (42)	0.09	3.1 ± 1.7 (27)	1.13
TRPP3_D523Q	-35.3 ± 12.5 (13)	0.25	3.3 ± 1.6 (8)	1.14
PKD1L_K2069D	-52.8 ± 11.9 (27)	0.13	4.5 ± 1.6 (15)	1.20

ΔE_{rev} is the change of reversal potential upon switching the bath solution from Na^+ to the test ions ($\Delta E_{rev} = E_{rev,X} - E_{rev,Na}$). Results are shown as mean and standard deviation. n = number of measurements. The reason that the relative permeability of TRPP3-D523Q channels to K^+ was similar to that of WT channels is because the D523Q mutation changed the reversible potential in both K^+ and Na^+ in the same direction and to a similar extent.

Supplementary Table S2. Data collection and refinement statistics.

	TRPP3- G699-W743
Data collection	
Space group	*P*321
Cell dimensions	
a, *b*, *c* (Å)	44.5, 44.5, 62.3
α, β, γ (°)	90, 90, 120
Resolution (Å)	20-2.8 (2.9-2.8) *
R_{sym} or R_{merge}	0.055(0.103)
$I/\sigma I$	36.7(25.2)
Completeness (%)	99.1(100)
Redundancy	9.0(9.2)
Refinement	
Resolution (Å)	20-2.8
No. reflections	1928
$R_{work/}$ R_{free}	0.235/0.286
No. atoms	
Protein	357
Ligand/ion	0
Water	44
B-factors	
Protein	46.9
Ligand/ion	0
Water	55.2
R.m.s deviations	
Bond lengths (Å)	0.013
Bond angles (º)	1.6

A single crystal was used for the dataset.
*Highest resolution shell is shown in parenthesis.